

Geophysical Research Letters

RESEARCH LETTER

10.1029/2018GL080579

Key Points:

- Timing of crystallization and exhumation of the youngest exposed plutons is constrained with high precision analytical techniques
- One of the highest exhumation rates for plutonic rocks worldwide is reported
- Exhumation of Pleistocene granitoid plutons is driven by subducting Izu-Bonin oceanic arc

Supporting Information:

- Supporting Information S1
- Data Set S1

Correspondence to:

C. J. Spencer,
cspencer@curtin.edu.au

Citation:

Spencer, C. J., Danišik, M., Ito, H., Hoiland, C., Tapster, S., Jeon, H., et al. (2019). Rapid exhumation of Earth's youngest exposed granites driven by subduction of an oceanic arc. *Geophysical Research Letters*, *46*, 1259–1267. <https://doi.org/10.1029/2018GL080579>

Received 20 SEP 2018

Accepted 12 JAN 2019

Accepted article online 18 JAN 2019

Published online 2 FEB 2019

Rapid Exhumation of Earth's Youngest Exposed Granites Driven by Subduction of an Oceanic Arc

C. J. Spencer¹ , M. Danišik², H. Ito³, C. Hoiland⁴ , S. Tapster⁵, H. Jeon^{6,7}, B. McDonald², and N. J. Evans^{1,2} 

¹Earth Dynamics Research Group, The Institute of Geoscience Research, School of Earth and Planetary Sciences, Curtin University, Perth, Western Australia, Australia, ²John de Laeter Centre, The Institute of Geoscience Research, Curtin University, Perth, Western Australia, Australia, ³Geosphere Science Sector, Central Research Institute of Electric Power Industry, Chiba, Japan, ⁴Department of Geological Sciences, Stanford University, Stanford, CA, USA, ⁵NERC Isotope Geosciences Facilities, British Geological Survey, Nottingham, UK, ⁶Centre for Microscopy, Characterisation and Analysis, University of Western Australia, Perth, Western Australia, Australia, ⁷Now at the Swedish Museum of Natural History, Stockholm, Sweden

Abstract Exhumation of plutonic systems is driven by a range of mechanisms including isostatic, tectonic, and erosional processes. Variable rates of plutonic exhumation in active subduction systems may be driven by idiosyncrasies of regional geology or by first-order tectonic features. We report new age, isotope, and low-temperature thermochronology constraints of granitoids from the Hida Mountains of central Japan that constrain the highest rates and magnitude of plutonic rock exhumation within the Japan and one of the highest worldwide. This extreme exhumation is centered on the apex of a lithospheric scale anticlinorium associated with the subduction of the Izu-Bonin oceanic arc. The spatial and temporal relationship between the exhumation of these Pleistocene plutons and the subducting/accreting Izu-Bonin oceanic arc links the plate-scale geodynamics and regional exhumation patterns. Identifying thermochronological anomalies within magmatic arcs provides an opportunity to identify ancient asperities previously subducted and responsible for rapid exhumation rates within ancient subduction systems.

Plain Language Summary Plutonic rocks reach the surface through a variety of geological processes. Generally, this is driven by active tectonic and erosive forces. We provide high-precision geochronological constraint on the youngest exposed subduction zone plutons found in the Hida Mountains of Japan that are 818.5 ± 9.6 thousand years old. Regionally, the Hida Mountains is identified as a thermochronological “hot spot” where the rocks in the region came to the surface very rapidly within the past ~300,000 years. The exhumation of these plutons was driven by the subduction of the Izu-Bonin oceanic arc.

1. Introduction

Rates of exhumation of plutonic rocks and processes controlling it vary for different tectonic settings (Herman et al., 2013). In cratonic regions that are characterized by long-term stability and little internal deformation, the exhumation of plutonic rocks is controlled primarily by erosion on the surface and exhumation rates are very low, typically not exceeding few tens of meters per million year (e.g., Danišik et al., 2008; Gleadow et al., 2002). Exhumation of plutonic rocks on plate boundaries, in contrast, is enhanced by tectonic processes whereby exhumation rates often range from several hundreds of meters to a few kilometers per million year (e.g., Danišik et al., 2007; Glotzbach et al., 2010; Thomson et al., 2001). It is often difficult to constrain whether high exhumation rates are achieved primarily through higher erosive potential due to topographic and climatic effects or are instead accomplished through structural mechanisms such as intraorogenic upper crustal extension and/or midcrustal isostatic readjustment, for example. Constraints on bedrock exhumation rates are critical in assessing these questions especially in modern settings where comparisons can be made to measurable precipitation rates, mass wasting flux, and surface uplift to better understand the nature of ancient orogenic processes.

The Hida Mountain Range (HMR) is unique in that it contains the youngest exposed plutonic rocks on the planet dated as young as 0.8 Ma (Ito et al., 2012, 2013). This fact together with reported cooling ages of <1 Ma (Yamada, 1999; Yamada & Harayama, 1999) requires extremely rapid exhumation rates, but why this is the

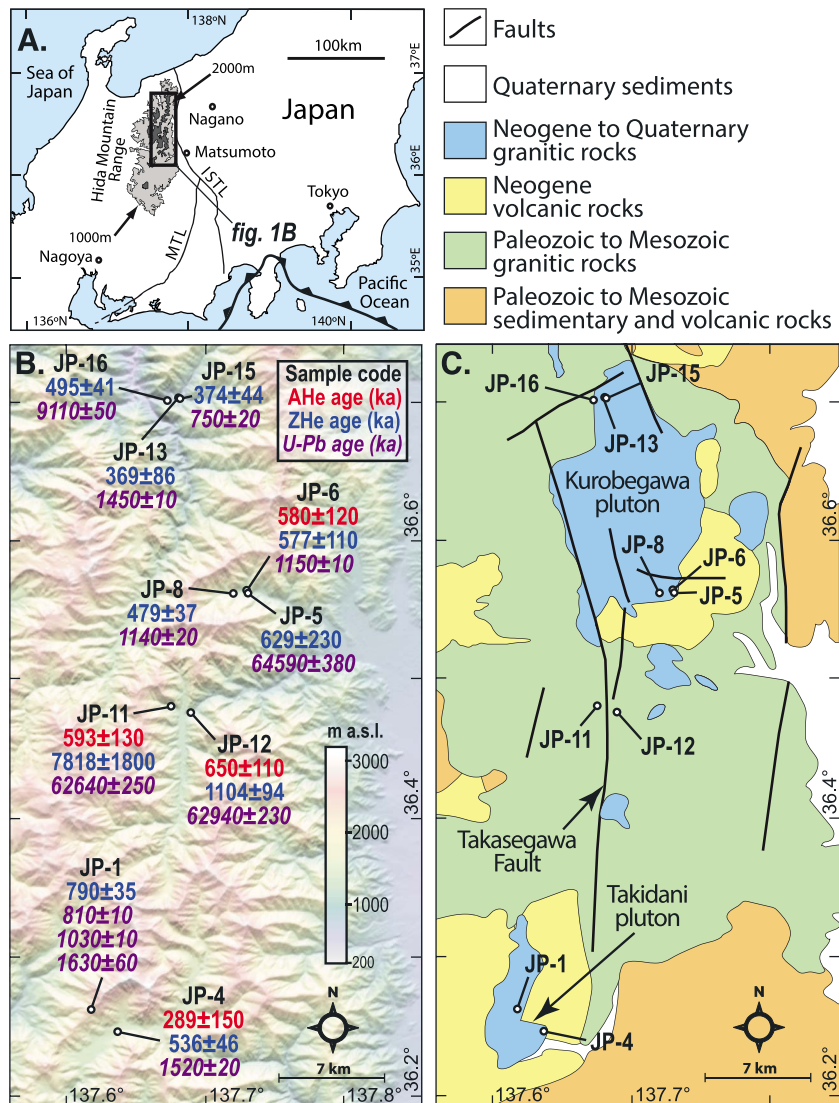


Figure 1. (a) Simplified map of the Hida Mountain Range (HMR; after Ito et al., 2017). ISTL = Itoigawa-Shizuoka Tectonic Line; MTL = Median Tectonic Line. (b) Topographic map of the sampling region of the HMR with sample locations and geochronological and thermochronological data from this study. All uncertainties are given at 2 sigma and include systematic uncertainty (2%). (c) Simplified geologic map of the HMR (after Ito et al., 2013).

case and how exhumation rates vary temporally and spatially in this region remains unresolved (Yamada & Harayama, 1999). The driver of this exhumation is thought to be associated with E-W compression accommodated by the Takasegawa fault that lies parallel to the Itoigawa-Shizuoka Tectonic Line (ISTL; Harayama, 2003; Harayama et al., 2003; Ito et al., 2012; Yamada, 1999). Additionally, the Philippine Sea plate is subducting obliquely to the direction of Pacific Plate convergence (Isozaki, 1996). However, the orientation of this major fault zone is parallel to the convergence direction and perpendicular to the major tectonic features associated with the Japanese subduction system (Figure 1). Thus, the nature of the structural features within and flanking the HMR and their relationship to boundary processes and subducting slab geometry and kinematics within the Japanese subduction zone is unclear.

Thermochronology can constrain the temperature-time histories of rocks so as to model the age and rate of their exhumation to the surface and to better constrain the geometry of structures that may have accommodated some or all of their exhumation. Low-temperature thermochronometers such as zircon and apatite (U-Th)/He systems are optimal for characterizing the upper few kilometers of exhumation

Table 1
Sample Information, Global Positioning Satellite (GPS) Localities, Geochronological and Thermochronological Summary, and Isotopic Data

Sample	Lithology	Latitude	Longitude	Zircon U-Pb age			(U-Th)/He age		Mineral	δ18O		εHF	
				Myr	± wtd 2σ	± sys 2σ	kyr	± 2σ		‰	± wtd 2σ	ε	± wtd 2σ
JP01.1	Granodiorite	36.26637	137.61926	1.63	0.06	0.25	790	35	zrn	rose			
JP01.2				1.03	0.01	0.10							
JP01.3				0.81	0.01	0.10							
JP04	Granodiorite	36.249733	137.637566	1.52	0.02	0.14	536	46	zrn	6.39	0.41	-1.83	0.29
										289	150	ap	
JP05	Granite	36.55995	137.72974	64.59	0.38	1.43	629	230	zrn	6.29	0.67	-2.99	0.28
JP06	Granite	36.56044	137.72932	1.15	0.01	0.10	601	130	zrn	5.90	0.40	-0.56	0.33
JP08	Granite	36.55959	137.71953	1.14	0.02	0.14	479	37	zrn	5.88	0.29	-1.03	0.28
JP11	Granite	36.4795	137.67508	62.64	0.25	1.35	7818	1800	zrn	6.91	0.20	-3.25	0.25
JP12	Granite	36.47516	137.68909	62.94	0.23	1.35	1104	94	zrn	6.79	0.37	-4.58	0.28
JP13	Granite	36.69868	137.68022	1.45	0.01	0.10	369	86	zrn				
JP15 (ICP-MS)	Aplite	36.69867	137.68069	0.75	0.02	0.14	374	44	zrn	6.02	0.16	2.42	0.29
JP15 (ID-TIMS)													
JP16	Granite	36.69636	137.67264	9.11	0.05	0.29	495	41	zrn	6.34	0.40	-0.43	0.28

Note. ICP-MS = inductively coupled plasma mass spectrometry; ID-TIMS = isotope dilution-thermal ionization mass spectrometry.

paths, whereas high-temperature systems such as zircon U-Pb method help to pinpoint beginning of the exhumation paths at magmatic temperatures.

In this study, we provide new zircon U-Pb geochronology together with zircon (U-Th)/He (ZHe) and apatite (U-Th)/He (AHe) thermochronological data from igneous bedrocks samples in the HMR that not only provide the most precise geochronology of the region (using isotope dilution-thermal ionization mass spectrometry) but also provide constraints on geodynamics of the formation, evolution, and exhumation of the plutonic systems of the HMR. These data provide further implications on spatial exhumation patterns of a complex subduction system that link the regional geology to tectonic plate scale geodynamic forcings.

2. Geological Setting and Samples

The HMR is one of the highest mountain systems in Japan. It includes several >3,000-m peaks and stretches north-south for over 100 km. The HMR lies west of the ISTL (i.e., the Eurasian-North American plate boundary) and is recognized as one of the most active seismotectonic regions of the Japanese islands (Ide, 2001; Mikumo et al., 1988). The HMR is composed predominately of Upper Cretaceous to lower Cenozoic plutonic rocks and Pleistocene to Holocene volcanic rocks with a minor amount of older pre-Cenozoic sedimentary and metamorphic basement. Within the HMR are two major Quaternary plutonic complexes, the Kurobegawa Granite and Takidani Granodiorite. The Kurobegawa granite pluton is exposed over an area of ~100 km² and represents the youngest exposed felsic plutonic complex in the world that has previously been dated at ~750 ka (Ito et al., 2017).

The Kurobegawa Granite has a vertical exposure from 700 to 3,000 m and is geochemically and texturally divided into three units (upper, middle, and lower) and is intrusive into the Quaternary Jiigatake felsic volcanic rocks (Harayama et al., 2003; Wada et al., 2004). Our sampling campaign targeted the northern and southern portions of the pluton. Samples, ranging in composition from diorite (enclaves) to granodiorite and granite, were collected from the locality previously identified as hosting the youngest granite plutonic sample on Earth (Ito et al., 2013). The zircon U-Pb ages of granodiorite samples reported by Ito et al. (2017) reproduce and confirm the young age previously reported (Harayama et al., 2010). However, one sample (JP15) was also collected from an aplite dyke that crosscuts the granodiorite previously argued to be the youngest granite.

The Takidani Granodiorite covers ~50 km² with vertical exposure from 1,450 to 2,670 m in elevation that is elongated along the N-S axis of the HMR. The pluton is compositionally zoned with equigranular biotite-

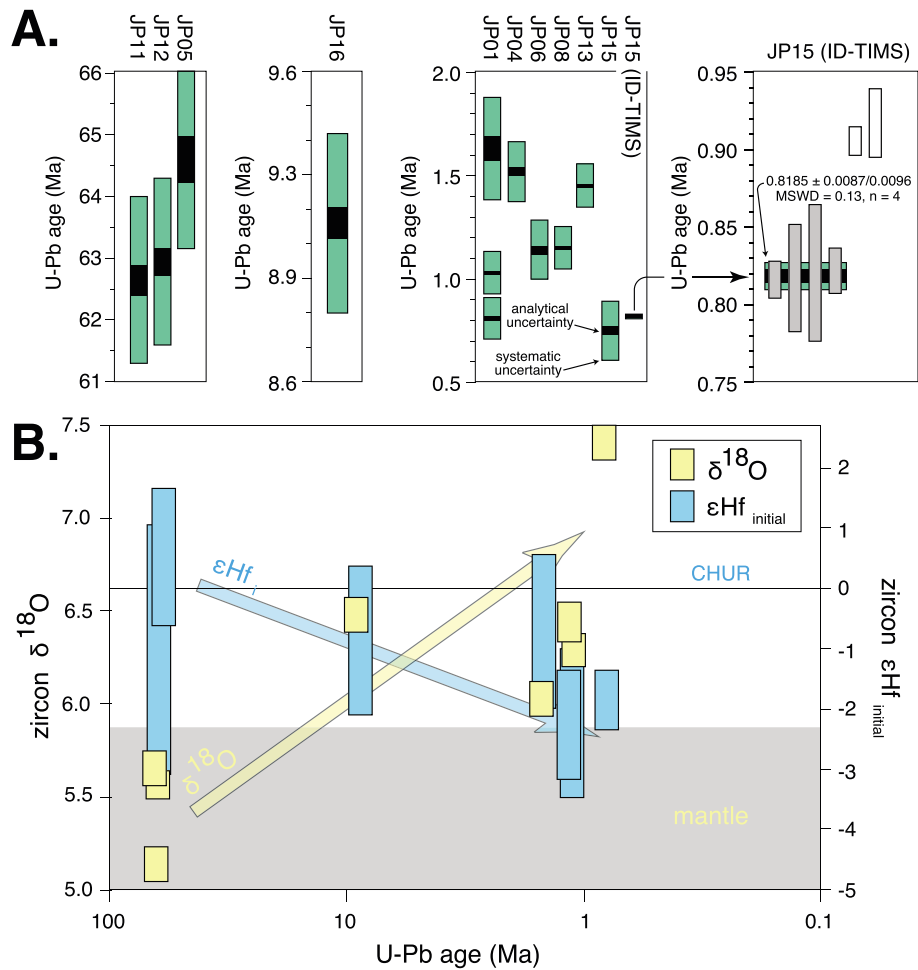


Figure 2. (a) Zircon U-Pb data from the Hida Mountain Range granitoid samples of Paleocene, Miocene, and Pleistocene age, respectively. All samples were analyzed with LA-ICP-MS, and JP15 was also analyzed by ID-TIMS. Sample JP01 had multiple age populations. (b) Zircon O- and Hf- isotope compositions (shown at 2 sigma) plotted against U-Pb age (note the log scale). Mantle $\delta^{18}O$ compositional range is from Page et al. (2007). ϵHf values are shown as initial ratios at time of crystallization ($\epsilon Hf_{initial}$). CHUR = chondrite uniform reservoir; LA-ICP-MS = laser ablation inductively coupled plasma mass spectrometry; ID-TIMS = isotope dilution-thermal ionization mass spectrometry.

hornblende granodiorite at the base grading toward porphyritic biotite-hornblende granite at the top (Harayama, 1992; Ito et al., 2017). Two samples were collected from the southern portions of the pluton. Additional samples of Miocene and Paleocene granites were collected within the environs of the Kurobegawa and Takidani plutons (Okukurobe and Oshirasawa). GPS coordinates of sample locations are presented in Table 1.

3. Methods

Collected samples were disaggregated using jaw crusher and disc mill housed at the John de Laeter Centre (JdLC) at Curtin University. Zircon and apatite were extracted using traditional mineral separation techniques (i.e., sieving, Wilfley table, Franz magnetic separation, and lithium polytungstate and diiodomethane heavy liquid separation). Zircon were mounted in epoxy, imaged with cathodoluminescence, and analyzed for $\delta^{18}O$, U-Pb, and Hf via secondary ion mass spectrometry ($\delta^{18}O$) at the University of Western Australia and laser ablation inductively coupled plasma mass spectrometry (LA-ICP-MS; U-Pb and Hf) at the JdLC following the methods of Spencer, Yakymchuk, and Ghaznavi (2017). Zircon from one sample (JP15) was analyzed with chemical abrasion-isotope dilution-thermal ionization mass spectrometry (CA-ID-TIMS) at the NERC Isotope Geosciences Laboratory of the British Geological Survey following the methods of Condon

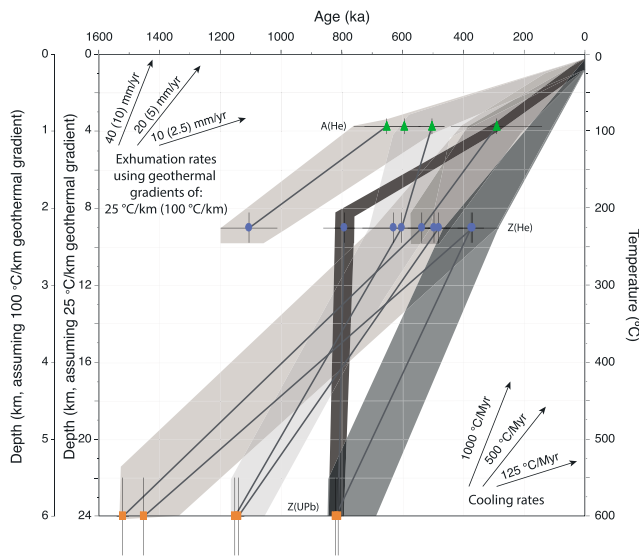


Figure 3. Time-temperature exhumation paths for the Hida Mountain Range granitoids as constrained by zircon and apatite geochronological/thermochronological data and assuming a geothermal gradient of 25 and 100 °C/km (Tanaka et al., 2004) and zircon crystallization of 600 °C, that is, the approximate minimum temperature of the granite wet solidus (Holtz & Johannes, 1994; Luth et al., 1964). If the true zircon crystallization temperature were higher, the exhumation rates would be higher and if the geothermal gradient were higher, the exhumation rates would be lower.

et al. (2015). Zircon and apatite were analyzed for (U-Th)/He using an Alphachron system and solution ICP-MS at the JdLC and TSW Analytical, respectively, following the methods of Danišik, Štěpančíková, and Evans (2012) and Danišik, Kuhlemann, et al. (2012). Full methodology is described in the supporting information. Summary of data in this study is presented in Table 1.

4. Results

4.1. Zircon U-Pb (LA-ICP-MS)

Ten samples were analyzed via LA-ICP-MS that range in age from ~0.8 to ~64.6 Ma (Figure 2a). Weighted means and reduced chi-square values were calculated using $KD\chi$ (Spencer, Cavošie, et al., 2017). Nine samples revealed single populations (as defined by the reduced chi-square test; Spencer et al., 2016), whereas one sample (JP01) revealed three discrete age populations (~1.4, ~1.0, and ~0.8 Ma). Weighted means of the samples fall into five discrete ages, ~0.8 Ma (two samples), ~1.0–1.2 Ma (three samples), ~1.5 Ma (three samples), ~9 Ma (one sample), and ~63 Ma (three samples).

4.2. Zircon U-Pb (CA-ID-TIMS)

Chemically abraded zircon (Mattinson, 2005) from sample JP15 analyzed by isotope dilution-thermal ionization mass spectrometry following the method of Tapster et al. (2016) yielded a ^{230}Th -corrected $^{206}\text{Pb}/^{238}\text{U}$ weighted mean age of $0.8185 \pm 0.0087/0.0096$ Ma (± 2 sigma analytical/total uncertainty; $n = 4$, Mean Square Weighted Deviation (MSWD) = 0.13) from the youngest population interpreted as best estimate for emplacement. Two additional grains yielded ages of ~0.9 Ma that were excluded from the weighted mean age calculation (Figure 2a). The ^{230}Th correction adds ~0.09 Ma (from 0.7282 ± 0.0030 to 0.8185 ± 0.0087) to the final age.

4.3. Zircon $\delta^{18}\text{O}$ and ϵ_{Hf}

Zircon $\delta^{18}\text{O}$ were obtained for eight samples with weighted means of $\delta^{18}\text{O}$ range from $5.9 \pm 0.4\text{‰}$ to $6.9 \pm 0.2\text{‰}$. When combined with the geochronological data, the $\delta^{18}\text{O}$ values increase from the Paleocene- to Quaternary-age samples (Figure 2b). Zircon ϵ_{Hf} was obtained for the same samples as $\delta^{18}\text{O}$ whose weighted means range from -0.4 ± 0.3 to -4.6 ± 0.3 and decrease through time (Figure 2b).

4.4. Zircon and Apatite (U-Th)/He

Single zircon grains ($n = 60$) from nine and apatite single grains ($n = 19$) from four samples were dated by (U-Th)/He method. Average zircon and apatite (U-Th)/He ages corrected for alpha ejection (Farley et al., 1996) range from ~7.8 Ma to ~370 kyr and from ~650 to ~289 kyr, respectively (Figure 1). See supporting information Figure S1 for modeled time-temperature diagrams showing thermal trajectories reproducing measured (U-Th)/He ages of the samples.

5. Discussion

Geochronologic data have previously been reported from the Kurobegawa and Takidani plutons highlighting the fact these plutons are the youngest currently known on the planet (Harayama, 1992, 1994; Ito et al., 2017, 2013; Yamada & Harayama, 1999). Previously published thermochronologic data of the Takidani pluton based on whole rock and biotite Rb-Sr, biotite and hornblende K-Ar, and zircon fission track dating methods also identified the HMR as representing a region of rapid exhumation (Harayama, 1992, 1994; Yamada & Harayama, 1999). The high-precision CA-ID-TIMS zircon U-Pb analyses of the youngest phase of magmatism of the Kurobegawa plutonic system support this with a final age of 818.5 ± 9.6 kyr (Figure 2). The Quaternary magmatism in the HMR appears to have occurred in three discrete pulses at ~2.3, ~1.6, and 0.9 Ma evidenced by analysis of detrital zircon in modern rivers (Ito et al., 2017). The LA-

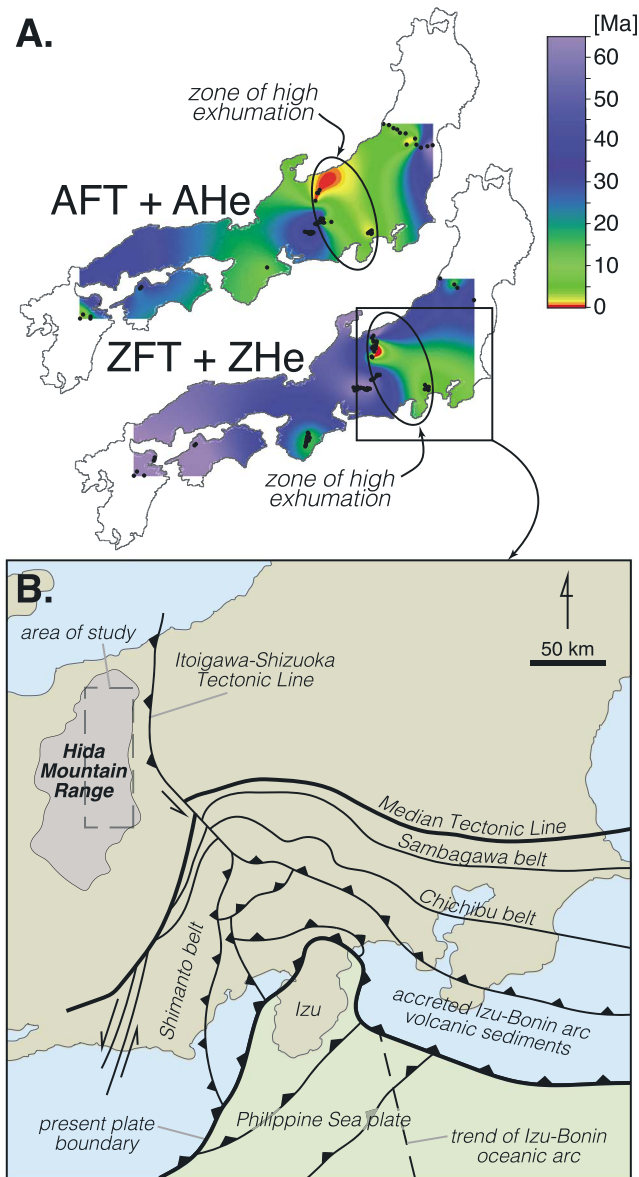


Figure 4. (a) Spatial interpolation (inverse distance weighting) of compiled zircon and apatite fission track (ZFT and AFT, respectively) and ZHe and AHe data from Japan. Volcanic and sedimentary samples are excluded from this compilation. There is a clear zone of high exhumation that is centered on the Hida Mountain Range (HMR). Data are compiled from Hasebe et al., 2000; Ito & Tanaka, 1999; Kamp & Takemura, 1993; Sueoka et al., 2012, 2017; Tagami & Shibata, 1993; Yamada & Harayama, 1999; Yamada & Tagami, 2008; Yuguchi et al., 2011, 2017; and this study. (b) Simplified map of the major tectonic structures of central Japan (Yamamoto et al., 2009). Importantly, these structures are either caused or heavily modified by the collision and accretion/subduction of the Izu-Bonin oceanic arc. The HMR lies directly in line with the trajectory of the Izu-Bonin oceanic arc that is likely the direct cause of the fast exhumation of the HMR. In all cases, the apatite He ages are younger than the zircon He ages. The apparent contradiction to this relationship seen in the regions without data is due to interpolation methods.

ICP-MS zircon U-Pb analyses also confirm the used ages of Quaternary pulses of magmatism as well as previous episodes of magmatism extending back to the early Paleogene (Figure 2).

The zircon $\delta^{18}\text{O}$ and ϵHf data presented herein provide insight into the genesis and evolution of the plutonic systems of the HMR. The oldest magmatism in the HMR displays moderately elevated $\delta^{18}\text{O}$ and unradiogenic ϵHf implying an elevated degree of reworking older crust (average depleted mantle model age = $\sim 1,200$ Ma). The ϵHf signatures subsequently decrease through time, and $\delta^{18}\text{O}$ increase through time, with the Paleocene phase of magmatism representing the most mantle-like $\delta^{18}\text{O}$ and most radiogenic ϵHf implying an increased amount of crustal recycling with time. This potentially signals the increased reworking of subducted supracrustal material from the Izu-Bonin Arc.

The new ZHe and AHe data constrain the timing of cooling of the samples through the ~ 225 and ~ 95 °C isotherms (assuming 60- μm radius equivalent sphere and the measured average cooling rate of 500 °C/km; Farley, 2002; Reiners et al., 2004), respectively, related to the exhumation of the plutons in the HMR. ZHe data suggest that central part of the range (sample JP12) reached the depths of ~ 3.0 km at 1.1 Ma (here and elsewhere the values were calculated by assuming a geothermal gradient of ~ 70 °C/km (average values from the HMR as reported by Tanaka et al., 2004, and surface temperature of 10 °C), whereas the northern and southern parts of the pluton at 790–370 kyr. AHe data suggest that central part of the pluton reached the depths of ~ 1.2 km at 650–580 kyr, and southern part arrived at ~ 1.2 -km depths at 290 kyr. These AHe ages document final exhumation of HMR plutons in the Middle Pleistocene and, together with two ages from Namche Barwa Syntaxis (Yang et al., 2018), represent the youngest cooling ages ever reported for basement rocks worldwide. The contrasting tectonic settings responsible for these exceptionally young cooling ages (oceanic subduction and continental collision) imply that the rapid exhumation rates are not confined to continent collisional settings.

High-temperature U-Pb and low-temperature (U-Th)/He data allow reconstruction of complete cooling trajectories for the samples from their crystallization to their exhumation to the surface (Figure 3), and the obtained cooling trajectories in combination with assumed geothermal gradients can be in turn used to calculate not only the rates but also the magnitude of exhumation. Our data for <1.6 Ma granites suggest that some portions of HMR plutons were exhumed from depths of <24 km to subsurface levels in 400 kyr at rates ranging from 20 up to 40 mm/year (km/Ma; assuming a minimum of 25 °C/km; 5 to 10 mm/year (km/Ma) if 100 °C/km is assumed; 25 and 100 °C/km are minimum and maximum values of geothermal gradient of the HMR reported by Tanaka et al., 2004). These extremely high exhumation rates and magnitudes are one of the greatest values thus far documented for granites by geochronological data. It is likely, however, that a portion of the extreme cooling paths documented between zircon U-Pb ages of crystallization and ZHe age reflects rapid initial cooling due to emplacement of the magma at relatively shallow depths and thus will need to be amended as future studies provide better constraints on emplacement depth.

Our new constraints can be compared to previous estimates of exhumation in the HMR and regionally. Terrestrial in situ cosmogenic nuclides

were previously used to estimate denudation rates in the HMR ranging from 0.2 to 7.0 mm/year (Matsushi et al., 2014), which are significantly lower than the exhumation rates presented in this study. This slight difference can be explained by the fact that cosmogenic nuclides record denudation moderated by surface processes rather than tectonic processes that are recorded by high- and low-temperature thermochronometers presented here (Vance et al., 2003). Maximum uplift in the HMR during the Quaternary was estimated to be approximately 1,700 m by measuring the elevation of low-relief erosional surfaces assumed to represent uplifted remnants of peneplains established by late Neogene time at near sea level (Research Group for Quaternary Tectonic Map, 1968). It is possible that the maximum uplift of ~1,700 m is underestimated because this study did not account for denudation and neglected the possibility of high-altitude denudation surfaces that were potentially formed by periglacial processes (Sugai, 1990, 1995). Low-temperature thermochronology data have also been used in southern part of the Northeast Japan Arc (Figure 4), to estimate exhumation rates as being <0.1 mm/year in the fore-arc region, ~0.1 to 1 mm/year along the volcanic front, and ~0.1 to 0.3 mm/year in the back-arc region (Sueoka et al., 2017).

The HMR lies parallel to the ISTL that is likely the primary fault system controlling the exhumation of the Quaternary plutonic rocks (Harayama, 1992; Ito et al., 2013; Wada, 2004). ISTL is a complex active thrust fault system that thrusts the crustal block of the HMR to the east (Sagiya et al., 2002, 2004). Slip rates along the thrust fault systems associated with the Itoigawa-Shizuoka Tectonic Line are estimated as high as ~9 mm/year (Ikeda & Yonekura, 1986).

Importantly, the ISTL lies along the apex of a large anticlinorium within the Izu collision zone (Figure 4). The collision of the Izu-Bonin arc with the Honshu arc has resulted in the deformation of the major tectonic boundaries in central Honshu and the subduction of the Izu-Bonin arc, and the buoyant nature of the subducting oceanic arc is likely the direct cause of the exhumation in the HMR (Yamamoto et al., 2009).

The spatially diverse exhumation of the Honshu arc (Figure 4) may provide a useful framework in constraining the subduction of crust thicker than normal oceanic crust (e.g., oceanic arcs, ocean islands, and mid-ocean ridges). We would predict that regions where thicker than normal oceanic crust has subduction would have experienced higher than normal exhumation. For example, the subduction of the Nazca Ridge beneath the Andes of South America has resulted in ~5-km exhumation of the Fitzcarrald Arch (Bishop et al., 2018; Espurt et al., 2010). Although the basement rocks are not yet exposed at the surface in the Fitzcarrald Arch, our model would predict the basement rocks beneath the sedimentary cover that would exhibit younger exhumation ages than the basement north and south where the Nazca Ridge is subducting.

Exhumation anomalies in subduction zones around the world merit further consideration for their potential as geothermal resources. Additionally, campaign-style thermochronological investigations of ancient subduction zones may provide insight into the reconstruction of the oceanic crust and whether exhumation “hot spots” as seen in the HMR indicate the subduction of thicker-than-normal oceanic crust.

Acknowledgments

The authors thank two anonymous reviewers for providing helpful and constructive comments. GeoHistory Facility instruments (part of the John de Laeter Centre) were funded via an Australian Geophysical Observing System (AGOS) grant provided to AuScope by the AQ44 Australian Education Investment Fund. The Australian Microscopy and Microanalysis Research Facility, AuScope, the Australian Science and Industry Endowment Fund, and the State Government of Western Australia contributed funding to Centre for Microscopy, Characterization, and Analysis at the University of Western Australia. M. D. was supported by the Australian Research Council (ARC) Discovery funding scheme (DP160102427), and C. S. and M. D. were supported by Curtin Research Fellowship. M. D. thanks C. May for help with solution ICP-MS analyses, I. Dunkl for sharing PepiFLEX software for ICP-MS data reduction, and A. Frew for help with mineral dissolution. The authors affirm that there is no real or perceived financial conflicts of interests. The full data set supporting the conclusions can be obtained in the supporting information.

References

- Bishop, B. T., Beck, S. L., Zandt, G., Wagner, L. S., Long, M. D., & Tavera, H. (2018). Foreland uplift during flat subduction: Insights from the Peruvian Andes and Fitzcarrald Arch. *Tectonophysics*, 731, 73–84.
- Condon, D. J., Schoene, B., McLean, N. M., Bowring, S. A., & Parrish, R. R. (2015). Metrology and traceability of U-Pb isotope dilution geochronology (EARTHTIME Tracer Calibration Part I). *Geochimica et Cosmochimica Acta*, 164, 464–480. <https://doi.org/10.1016/j.gca.2015.05.026>
- Danišik, M., Kuhlemann, J., Dunkl, I., Evans, N. J., Székely, B., & Frisch, W. (2012). Survival of ancient landforms in a collisional setting as revealed by combined fission track and (U-Th)/He thermochronometry: A case study from Corsica (France). *The Journal of Geology*, 120(2), 155–173. <https://doi.org/10.1086/663873>
- Danišik, M., Kuhlemann, J., Dunkl, I., Székely, B., & Frisch, W. (2007). Burial and exhumation of Corsica (France) in the light of fission track data. *Tectonics*, 26, TC1001. <https://doi.org/10.1029/2005TC001938>
- Danišik, M., Sachsenhofer, R. F., Privalov, V. A., Panova, E. A., Frisch, W., & Spiegel, C. (2008). Low-temperature thermal evolution of the Azov Massif (Ukrainian Shield – Ukraine)—Implications for interpreting (U-Th)/He and fission track ages from cratons. *Tectonophysics*, 456(3–4), 171–179. <https://doi.org/10.1016/j.tecto.2008.04.022>
- Danišik, M., Štěpánčíková, P., & Evans, N. J. (2012). Constraining long-term denudation and faulting history in intraplate regions by multisystem thermochronology: An example of the Sudetic Marginal Fault (Bohemian Massif, central Europe). *Tectonics*, 31, TC2003. <https://doi.org/10.1029/2011TC003012>
- Espurt, N., Baby, P., Brusset, S., Roddaz, M., Hermoza, W., & Barbarand, J. (2010). The Nazca Ridge and uplift of the Fitzcarrald Arch: Implications for regional geology in northern South America. In *Amazonia, Landscape and Species Evolution: A Look into the Past* (pp. 89–100). Oxford: Blackwell-Wiley.
- Farley, K. A. (2002). (U-Th)/He dating: Techniques, calibrations, and applications. *Reviews in Mineralogy and Geochemistry*, 47(1), 819–844. <https://doi.org/10.2138/rmg.2002.47.18>

- Farley, K. A., Wolf, R. A., & Silver, L. T. (1996). The effects of long alpha-stopping distances on (U-Th)/He ages. *Geochimica et Cosmochimica Acta*, 60(21), 4223–4229. [https://doi.org/10.1016/S0016-7037\(96\)00193-7](https://doi.org/10.1016/S0016-7037(96)00193-7)
- Gleadow, A. J. W., Kohn, B. P., Brown, R. W., O'Sullivan, P. B., & Raza, A. (2002). Fission track thermotectonic imaging of the Australian continent. *Tectonophysics*, 349(1–4), 5–21. [https://doi.org/10.1016/S0040-1951\(02\)00043-4](https://doi.org/10.1016/S0040-1951(02)00043-4)
- Glottzbach, C., Reinecker, J., Danišik, M., Rahn, M., Frisch, W., & Spiegel, C. (2010). Thermal history of the central Gotthard and Aar massifs, European Alps: Evidence for steady state, long-term exhumation. *Journal of Geophysical Research*, 115, F03017. <https://doi.org/10.1029/2009JF001304>
- Harayama, S. (1992). Youngest exposed granitoid pluton on Earth: Cooling and rapid uplift of the Pliocene-Quaternary Takidani Granodiorite in the Japan Alps, central Japan. *Geology*, 20(7), 657–660. [https://doi.org/10.1130/0091-7613\(1992\)020<0657:YEGPOE>2.3.CO;2](https://doi.org/10.1130/0091-7613(1992)020<0657:YEGPOE>2.3.CO;2)
- Harayama, S. (2003). Quaternary and Pliocene granites in the Northern Japan Alps. In Hutton Symposium V, Field Guidebook.
- Harayama, S., Ohyabu, K., Miyama, Y., Adachi, H., & Shukuwa, R. (2003). Eastward tilting and uplifting after the late Early Pleistocene in the eastern-half area of the Hida Mountain Range. *The Quaternary Research (Daiyonki-Kenkyu)*, 42(3), 127–140. <https://doi.org/10.4116/jaqua.42.127>
- Harayama, S., Takahashi, M., Shukuwa, R., Itaya, T., & Yagi, K. (2010). High-temperature hot springs and Quaternary Kurobegawa Granite along the Kurobegawa River. *Journal of the Geological Society of Japan*, 116, 63–81.
- Hasebe, N., Suwargadi, B. W., & Nishimura, S. (2000). Fission track ages of the Omine acidic rocks, Kii Peninsula, Southwest Japan. *Geochemical Journal*, 34(3), 229–235. <https://doi.org/10.2343/geochemj.34.229>
- Herman, F., Seward, D., Valla, P. G., Carter, A., Kohn, B., Willett, S. D., & Ehlers, T. A. (2013). Worldwide acceleration of mountain erosion under a cooling climate. *Nature*, 504(7480), 423–426. <https://doi.org/10.1038/nature12877>
- Holtz, F., & Johannes, W. (1994). Maximum and minimum water contents of granitic melts: Implications for chemical and physical properties of ascending magmas. *Lithos*, 32(1–2), 149–159. [https://doi.org/10.1016/0024-4937\(94\)90027-2](https://doi.org/10.1016/0024-4937(94)90027-2)
- Ide, S. (2001). Complex source processes and the interaction of moderate earthquakes during the earthquake swarm in the Hida Mountains, Japan, 1998. *Tectonophysics*, 334(1), 35–54. [https://doi.org/10.1016/S0040-1951\(01\)00027-0](https://doi.org/10.1016/S0040-1951(01)00027-0)
- Ikeda, Y., & Yonekura, N. (1986). Determination of late Quaternary rates of net slip on two major fault zones in central Japan. *Bulletin of the Department of Geography, University of Tokyo*, 18, 49–63.
- Isozaki, Y. (1996). Anatomy and genesis of a subduction-related orogen: A new view of geotectonic subdivision and evolution of the Japanese Islands. *Island Arc*, 5(3), 289–320. <https://doi.org/10.1111/j.1440-1738.1996.tb00033.x>
- Ito, H., Spencer, C. J., Danišik, M., & Hoiland, C. W. (2017). Magmatic tempo of Earth's youngest exposed plutons as revealed by detrital zircon U-Pb geochronology. *Scientific Reports*, 7(1), 12,457. <https://doi.org/10.1038/s41598-017-12790-w>
- Ito, H., Tamura, A., Morishita, T., & Arai, S. (2012). Timing of some plutonic intrusions and tectonics in the Hida Mountain Range: An application of LA-ICP-MS U-Pb dating on zircons. *Journal of the Geological Society of Japan*, 118(7), 449–456. <https://doi.org/10.5575/geosoc.2012.0014>
- Ito, H., & Tanaka, K. (1999). Radiometric age determination on some granitic rocks in the Hida Range, central Japan. Remarkable age difference across a fault. *Geological Journal*, 105(4), 241–246.
- Ito, H., Yamada, R., Tamura, A., Arai, S., Horie, K., & Hokada, T. (2013). Earth's youngest exposed granite and its tectonic implications: The 10–0.8 Ma Kurobegawa Granite. *Scientific Reports*, 3, 1–5.
- Kamp, P. J., & Takemura, K. (1993). Thermo-tectonic history of Ryoke Basement in Hohi volcanic zone, northeast Kyushu, Japan: Constraints from fission track thermochronology. *Island Arc*, 2(4), 213–227. <https://doi.org/10.1111/j.1440-1738.1993.tb00088.x>
- Luth, W. C., Jahns, R. H., & Tuttle, O. F. (1964). The granite system at pressures of 4 to 10 kilobars. *Journal of Geophysical Research*, 69, 759–773. <https://doi.org/10.1029/JZ069i004p00759>
- Matsushi, Y., Matsuzaki, H., & Chigira, M. (2014). Determining long-term sediment yield from mountainous watersheds by terrestrial cosmogenic nuclides. *Journal of the Japan Society of Engineering Geology*, 54, 272–280. (in Japanese with English abstract)
- Mattinson, J. M. (2005). Zircon U-Pb chemical abrasion (“CA-TIMS”) method: Combined annealing and multi-step partial dissolution analysis for improved precision and accuracy of zircon ages. *Chemical Geology*, 220(1–2), 47–66. <https://doi.org/10.1016/j.chemgeo.2005.03.011>
- Mikumo, T., Wada, H., & Makoto, K. (1988). Seismotectonics of the Hida region, central Honshu, Japan. *Tectonophysics*, 147(1–2), 95–119. [https://doi.org/10.1016/0040-1951\(88\)90150-3](https://doi.org/10.1016/0040-1951(88)90150-3)
- Page, F. Z., Fu, B., Kita, N. T., Fournelle, J., Spicuzza, M. J., Schulze, D. J., et al. (2007). Zircons from kimberlite: New insights from oxygen isotopes, trace elements, and Ti in zircon thermometry. *Geochimica et Cosmochimica Acta*, 71(15), 3887–3903. <https://doi.org/10.1016/j.gca.2007.04.031>
- Reiners, P. W., Spell, T. L., Nicolescu, S., & Zanetti, K. A. (2004). Zircon (U-Th)/He thermochronometry: He diffusion and comparisons with ⁴⁰Ar/³⁹Ar dating. *Geochimica et Cosmochimica Acta*, 68(8), 1857–1887. <https://doi.org/10.1016/j.gca.2003.10.021>
- Research Group for Quaternary Tectonic Map (1968). Quaternary tectonic map of Japan, *Quaternary Research (Daiyonki Kenkyu)*, 7, 182–187 (in Japanese with English abstract).
- Sagiya, T., Nishimura, T., & Iio, Y. (2004). Heterogeneous crustal deformation along the central-northern Itoigawa-Shizuoka tectonic line fault system, central Japan. *Earth, Planets and Space*, 56(12), 1247–1252. <https://doi.org/10.1186/BF03353347>
- Sagiya, T., Nishimura, T., Iio, Y., & Tada, T. (2002). Crustal deformation around the northern and central Itoigawa-Shizuoka tectonic line. *Earth, Planets and Space*, 54(11), 1059–1063. <https://doi.org/10.1186/BF03353302>
- Spencer, C. J., Cavosie, A. J., Raub, T. D., Rollinson, H., Jeon, H., Searle, M. P., et al., & the Edinburgh Ion Microprobe Facility (EIMF) (2017). Evidence for melting mud in Earth's mantle from extreme oxygen isotope signatures in zircon. *Geology*, 45(11), 975–978. <https://doi.org/10.1130/G39402.1>
- Spencer, C. J., Kirkland, C. L., & Taylor, R. J. M. (2016). Strategies towards statistically robust interpretations of in situ U-Pb zircon geochronology. *Geoscience Frontiers*, 7(4), 581–589. <https://doi.org/10.1016/j.gsf.2015.11.006>
- Spencer, C. J., Yakymchuk, C., & Ghaznavi, M. (2017). Visualising data distributions with kernel density estimation and reduced chi-squared statistic. *Geoscience Frontiers*, 8(6), 1247–1252. <https://doi.org/10.1016/j.gsf.2017.05.002>
- Sueoka, S., Kohn, B. P., Tagami, T., Tsutsumi, H., Hasebe, N., Tamura, A., & Arai, S. (2012). Denudation history of the Kiso Range, central Japan, and its tectonic implications: Constraints from low-temperature thermochronology. *Island Arc*, 21(1), 32–52. <https://doi.org/10.1111/j.1440-1738.2011.00789.x>
- Sueoka, S., Tagami, T., & Kohn, B. P. (2017). First report of (U-Th)/He thermochronometric data across Northeast Japan Arc: Implications for the long-term inelastic deformation Crustal Dynamics: Unified Understanding of Geodynamics Processes at Different Time and Length Scales Yoshihisa Iio, Richard. *Earth, Planets and Space*, 69(1), 79.

- Sugai, T. (1990). The origin and geomorphic characteristics of the erosional low-relief surfaces in the Akaishi Mountains and the southern part of the Mikawa plateau, central Japan. *Geographical Review of Japan A*, 63(12), 793–813. https://doi.org/10.4157/grj1984a.63.12_793
- Sugai, T. (1995). Origin of the low-relief surfaces on ridges in the Kiso range and northern part of the Mino-Mikawa plateau, central Japan. Proceedings of the Department of Humanities, College of General Education, University of Tokyo. *Series of Human Geography*, 7, 1–40.
- Tagami, T., & Shibata, K. (1993). Fission track ages on some Ryoke granitic rocks along the Median Tectonic Line, Southwest Japan. *Geochemical Journal*, 27(6), 403–406. <https://doi.org/10.2343/geochemj.27.403>
- Tanaka, A., Yamano, M., Yano, Y., & Sasada, M. (2004). Geothermal gradient and heat flow data in and around Japan (I): Appraisal of heat flow from geothermal gradient data. *Earth, Planets and Space*, 56(12), 1191–1194. <https://doi.org/10.1186/BF03353339>
- Tapster, S., Condon, D. J., Naden, J., Noble, S. R., Petterson, M. G., Roberts, N. M. W., et al. (2016). Rapid thermal rejuvenation of high-crystallinity magma linked to porphyry copper deposit formation; evidence from the Koloula Porphyry Prospect, Solomon Islands. *Earth and Planetary Science Letters*, 442, 206–217. <https://doi.org/10.1016/j.epsl.2016.02.046>
- Thomson, S. N., Hervé, F., & Stöckhert, B. (2001). Mesozoic-Cenozoic denudation history of the Patagonian Andes (southern Chile) and its correlation to different subduction processes. *Tectonics*, 20, 693–711. <https://doi.org/10.1029/2001TC900013>
- Vance, D., Bickle, M., Ivy-Ochs, S., & Kubik, P. W. (2003). Erosion and exhumation in the Himalaya from cosmogenic isotope inventories of river sediments. *Earth and Planetary Science Letters*, 206(3–4), 273–288. [https://doi.org/10.1016/S0012-821X\(02\)01102-0](https://doi.org/10.1016/S0012-821X(02)01102-0)
- Wada, H. (2004). Mafic enclaves densely concentrated in the upper part of a vertically zoned felsic magma chamber: The Kurobegawa granitic pluton. *Hida Mountain Range, central Japan*, 7, 788–801.
- Wada, H., Harayama, S., & Yamaguchi, Y. (2004). Mafic enclaves densely concentrated in the upper part of a vertically zoned felsic magma chamber: The Kurobegawa granitic pluton, Hida Mountain Range, central Japan. *Bulletin of the Geological Society of America*, 116(7), 788–801. <https://doi.org/10.1130/B25287.1>
- Yamada, K., & Tagami, T. (2008). Postcollisional exhumation history of the Tanzawa Tonalite Complex, inferred from (U-Th)/He thermochronology and fission track analysis. *Journal of Geophysical Research*, 113, B03402. <https://doi.org/10.1029/2007JB005368>
- Yamada, R. (1999). Cooling history analysis of granitic rock in the Northern Alps, central Japan. *The Earth Monthly*, 21, 803–810.
- Yamada, R., & Harayama, S. (1999). Fission track and K-Ar dating on some granitic rocks of the Hida Mountain Range, central Japan. *Geochemical Journal*, 33(1), 59–66. <https://doi.org/10.2343/geochemj.33.59>
- Yamamoto, S., Senshu, H., Rino, S., Omori, S., & Maruyama, S. (2009). Granite subduction: Arc subduction. *Tectonic Erosion and Sediment Subduction*, 15, 443–453. <https://doi.org/10.1016/j.gr.2008.12.009>
- Yang, R., Herman, F., Fellin, M. G., & Maden, C. (2018). Exhumation and topographic evolution of the Namche Barwa Syntaxis, eastern Himalaya. *Tectonophysics*, 722, 43–52. <https://doi.org/10.1016/j.tecto.2017.10.026>
- Yuguchi, T., Amano, K., Tsuruta, T., Danhara, T., & Nishiyama, T. (2011). Thermochronology and the three-dimensional cooling pattern of a granitic pluton: An example from the Toki granite, Central Japan. *Contributions to Mineralogy and Petrology*, 162(5), 1063–1077. <https://doi.org/10.1007/s00410-011-0640-5>
- Yuguchi, T., Sueoka, S., Iwano, H., Danhara, T., Ishibashi, M., Sasao, E., & Nishiyama, T. (2017). Spatial distribution of the apatite fission-track ages in the Toki granite, central Japan: Exhumation rate of a Cretaceous pluton emplaced in the East Asian continental margin. *Island Arc*, 26(6), e12219. <https://doi.org/10.1111/iar.12219>